

## Modeling of Subsurface Throughflow in Urban Pervious Areas

Nielsen, Kristoffer T.; Nielsen, Jesper E.; Uggerby, Mads; Rasmussen, Michael R.

*Published in:*  
Journal of Hydrologic Engineering

*DOI (link to publication from Publisher):*  
[10.1061/\(ASCE\)HE.1943-5584.0001990](https://doi.org/10.1061/(ASCE)HE.1943-5584.0001990)

*Creative Commons License*  
CC BY 4.0

*Publication date:*  
2020

*Document Version*  
Publisher's PDF, also known as Version of record

[Link to publication from Aalborg University](#)

*Citation for published version (APA):*  
Nielsen, K. T., Nielsen, J. E., Uggerby, M., & Rasmussen, M. R. (2020). Modeling of Subsurface Throughflow in Urban Pervious Areas. *Journal of Hydrologic Engineering*, 25(12), Article 04020050.  
[https://doi.org/10.1061/\(ASCE\)HE.1943-5584.0001990](https://doi.org/10.1061/(ASCE)HE.1943-5584.0001990)

### General rights

Copyright and moral rights for the publications made accessible in the public portal are retained by the authors and/or other copyright owners and it is a condition of accessing publications that users recognise and abide by the legal requirements associated with these rights.

- Users may download and print one copy of any publication from the public portal for the purpose of private study or research.
- You may not further distribute the material or use it for any profit-making activity or commercial gain
- You may freely distribute the URL identifying the publication in the public portal -

### Take down policy

If you believe that this document breaches copyright please contact us at [vbn@aub.aau.dk](mailto:vbn@aub.aau.dk) providing details, and we will remove access to the work immediately and investigate your claim.

# Modeling of Subsurface Throughflow in Urban Pervious Areas

Kristoffer T. Nielsen, Ph.D.<sup>1</sup>; Jesper E. Nielsen, Ph.D.<sup>2</sup>; Mads Uggerby<sup>3</sup>; and Michael R. Rasmussen, Ph.D.<sup>4</sup>

**Abstract:** Infiltration excess runoff, i.e., runoff as a result of the rainfall intensity exceeding the infiltration capacity of the soil surface, has traditionally been considered the only contributor to the surface runoff from urban pervious areas. However, recent studies show that subsurface throughflow also can be a significant contributor to urban stormwater runoff. Although rainfall-runoff from urban pervious areas can contribute with large quantities of runoff, only little knowledge exists on this topic. In this study, experimental field observations of subsurface throughflow from the literature are used to assess the capability of different models to simulate this type of runoff. It is investigated how well three new modeling approaches in urban drainage engineering (linear reservoir, regression, and shallow neural network models) performs in simulating subsurface throughflow compared to two commonly used models (the time-area and kinematic wave model). The models are compared with the measured runoff rate and evaluated by the root mean square error (RMSE), Nash-Sutcliffe efficiency (NSE), and Bayesian likelihood ( $L$ ). Generally, a neural network containing 60 neurons and using up to 180 min of data back in time produces the best results (RMSE =  $0.59 \text{ L min}^{-1}$ , NSE = 0.91, and  $L = 0.92$ ). However, both the kinematic wave (RMSE =  $1.06 \text{ L min}^{-1}$ , NSE = 0.71, and  $L = 0.76$ ) and linear reservoir model (RMSE =  $0.98 \text{ L min}^{-1}$ , NSE = 0.75, and  $L = 0.78$ ) generate reasonable results despite their significantly simpler modeling approaches. DOI: 10.1061/(ASCE)HE.1943-5584.0001990. This work is made available under the terms of the Creative Commons Attribution 4.0 International license, <https://creativecommons.org/licenses/by/4.0/>.

**Author keywords:** Subsurface throughflow; Pervious surfaces; Linear reservoir model Kinematic wave; Neural network; Urban drainage; Stormwater runoff.

## Introduction

Rainfall-runoff from urban pervious areas can be an important runoff contributor to urban drainage networks. Therefore, high-quality runoff models are essential to sustain a good quality of urban drainage design. However, rainfall-runoff from pervious areas depends on a large variety of physical properties, which leads to a considerable spatial variation depending on the underlying physical properties of the pervious surface. Rainfall-runoff from urban pervious areas depends on factors such as vegetation cover, soil water conditions, soil structure, and morphological characteristics (Gregory 2006; Groenendyk et al. 2015; Jacobs et al. 2003; Pan and Shangguan 2006; Quinton et al. 1997; Sharma 1986). Furthermore, urban soils are often prone to high soil compaction due to the load of construction vehicles, which reduces the infiltration capacity (Gregory 2006). Due to the many physical variables affecting the pervious surface runoff, modeling the runoff is often associated

with a high degree of uncertainty. Additionally, data for precise surface and soil characterization and model calibration is rarely available to minimize the uncertainty. Therefore, there is a need for more knowledge on how runoff from urban pervious areas should be quantified and how it affects the capacity of urban drainage systems.

In urban drainage engineering, runoff from pervious areas is typically estimated based on the assumptions of infiltration excess overland flow where runoff is produced because the rainfall intensity exceeds the infiltration capacity of the soil surface, as drawn in the conceptual illustration in Fig. 1(a) (Green and Ampt 1911; Horton 1939). Under this assumption, runoff only occurs if the rainfall intensity exceeds the infiltration capacity of the surface. However, Pilgrim et al. (1978) found that subsurface throughflow (horizontal water transport in the soil close to the soil surface) and saturation excess overland flow (runoff directly on the surface of saturated soils) also contribute to runoff through the general processes conceptualized in Figs. 1(b and c). Several studies from rural and urban areas even found that subsurface throughflow and saturation excess runoff were the only contributors to runoff and that infiltration excess overland flow was absent (Dunne and Black 1970a; Dunne and Black 1970b; Kirkby and Chorley 1967; Nielsen et al. 2019). Therefore, infiltration excess overland flow should only be considered a subprocess in a runoff generation from pervious areas, and all runoff types must be considered in a holistic approach taking into consideration the site-specific surface and soil properties.

In urban drainage modeling, rainfall-runoff is typically estimated by the coupling of infiltration and surface runoff models. Richard's equation (Celia et al. 1990) is the most complex infiltration model, and due to its complexity, simplified models are often used in urban drainage engineering. The most widely used models

<sup>1</sup>Industrial Researcher, Dept. of Civil Engineering, Aalborg Univ., Thomas Manns Vej 23, Aalborg 9220, Denmark; EnviDan A/S, Vejlsøvej 23, Silkeborg 8600, Denmark (corresponding author). ORCID: <https://orcid.org/0000-0001-8720-832X>. Email: [kri@envidan.dk](mailto:kri@envidan.dk); [kni@civil.aau.dk](mailto:kni@civil.aau.dk)

<sup>2</sup>Associate Professor, Dept. of Civil Engineering, Aalborg Univ., Thomas Manns Vej 23, Aalborg 9220, Denmark.

<sup>3</sup>Head of Research and Development, EnviDan A/S, Vejlsøvej 23, Silkeborg 8600, Denmark.

<sup>4</sup>Professor with Specific Responsibilities, Dept. of Civil Engineering, Aalborg Univ., Thomas Manns Vej 23, Aalborg 9220, Denmark.

Note. This manuscript was submitted on April 5, 2019; approved on May 7, 2020; published online on September 17, 2020. Discussion period open until February 17, 2021; separate discussions must be submitted for individual papers. This paper is part of the *Journal of Hydrologic Engineering*, © ASCE, ISSN 1084-0699.

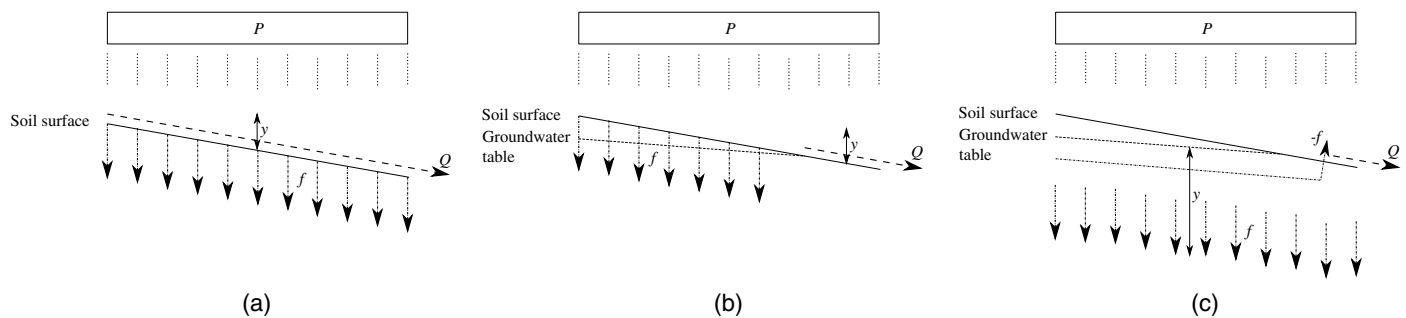


**Fig. 1.** Conceptual drawings of (a) infiltration excess overland flow; (b) saturation excess runoff; and (c) subsurface throughflow.  $P$  = precipitation;  $y$  = water depth of ponding water on the soil surface or within the soil;  $f$  = infiltration capacity; and  $Q$  = resulting runoff.

are the Green-Ampt model (Green and Ampt 1911) and Horton's equation (Horton 1939). These models require a relatively simple parametric input and are computationally more efficient than Richard's equation. Generally, infiltration models are coupled with hydrodynamic overland flow models. Surface runoff models also have different degrees of complexity whereas the Saint-Venant equations for two-dimensional overland flow are typically the most complex models used (Tayfur et al. 1993). This type of model is computationally demanding and is therefore primarily used for overland flow studies with limited geographical scale and time extent. In modeling urban drainage networks for long-term rainfall statistics, simplified surface runoff models are typically used, such as the kinematic wave approximation or time-area method (Butler and Davies 2004; Morris and Woolhiser 1980).

Current methods for modeling runoff from urban pervious surfaces implies that water either infiltrates vertically through the surface or discharges horizontally on the surface. However, this is conceptually not valid for subsurface throughflow because both vertical and horizontal water transport is present in the soil. In such cases, the optimal solution could be a two-dimensional numerical Darcy model, which is often used for soil water transport studies in rural and nonurban areas. With this modeling approach, both the horizontal and vertical water transport would be included physically in one model (Rassam et al. 2003). However, this model type is rarely used to simulate runoff from urban pervious areas. Therefore, traditional urban overland flow and infiltration models might not be the most suitable models based on current assumptions. Under these conditions, soil water transport models, such as simple subsurface throughflow models or linear reservoir models, can potentially be more accurate in modeling the correct runoff processes (Kirkby and Chorley 1967; Pedersen et al. 1980). Additionally, machine learning techniques, such as neural network models, could be an alternative by utilizing the inherent relationships in experimental data between soil hydrological properties and runoff (ASCE Task Committee on Application of Artificial Neural Networks in Hydrology 2000; Govindaraju 2000).

This study investigates three new methods for modeling runoff from urban pervious areas. The models are a linear reservoir model, regression models, and neural network models. For a standard of reference, the time-area method and kinematic wave model are used as these are traditionally used in urban drainage modeling. The scope is to evaluate frequently used models and their applicability in urban drainage engineering to model subsurface throughflow. The runoff models are calibrated based on field-scale measurements of a pervious urban area where subsurface throughflow was the dominant contributor to runoff. The performance of the models is compared, and their future applicability is discussed.

## Materials and Methods

Rainfall-runoff processes were measured with the field station described by Nielsen et al. (2019) located in Lystrup, Denmark. The field station collects runoff from a 4,300-m<sup>2</sup> grass covered urban catchment with a slope of 8.8%. The field station simultaneously measures the soil water content, soil matric potential, rainfall, and surface runoff. Surface runoff produced from different runoff processes is collected in a trench drain, as seen in Fig. 2(a), located at the outlet of the catchment presented in Fig. 2. The runoff rate is monitored with a V-notch weir [Fig. 2(b)] and afterwards discharged to the drainage system.

Soil volumetric water content and matric potential are measured in three sensor clusters, as shown in the schematic drawing in Fig. 3. The soil sensors are mounted in 10 cm of soil depth. Rainfall is measured with a tipping bucket rain gauge. The soil is characterized as a sandy loam according to the USDA soil classification system (Ashman and Puri 2013). Furthermore, there seems to be an increase in silt and clay particles in depths of 46 cm. The topsoil has a saturated hydraulic conductivity of 1.1 mm min<sup>-1</sup> (Nielsen et al. 2019).

Rainfall-runoff was monitored from September 2016 until July 2018. Within the measurement period, 63 days with runoff was recorded of which 53 days were due to periods of rainfall, and 10 days were due to a period of snowmelt. Runoff related to rainfall is divided into six rainfall-runoff events, all of which was recorded during fall and winter under high soil water content conditions. The rainfall-runoff events are divided based on the time in which measured runoff starts and stops. The result of this is that the rainfall-runoff events become significantly longer than any of the actual rainfall events. Instead, several rainfall events may occur within one rainfall-runoff event in this study. The period of snowmelt is not included in these rainfall-runoff events as this is a very different hydrological process. Therefore, 53 days of runoff is included in total in this model study.

None of the runoff-causing rainfall events exceeded the measured saturated infiltration capacity of the topsoil. On the contrary, runoff was more sensitive to high soil volumetric water content and, thereby, the water storage capacity of the soil. Prolonged periods of runoff while there is no active rainfall, combined with an inherent high soil volumetric water content, indicate that runoff from the area is comparable to subsurface throughflow. This resulted in exfiltration from the soil toward the soil surface at the bottom of the studied hill slope (Nielsen et al. 2019). Additionally, shorter periods of saturation excess runoff were present during rainfall as rainfall were unable to infiltrate in the areas where subsurface throughflow exfiltrated from the soil. This resulted in short term

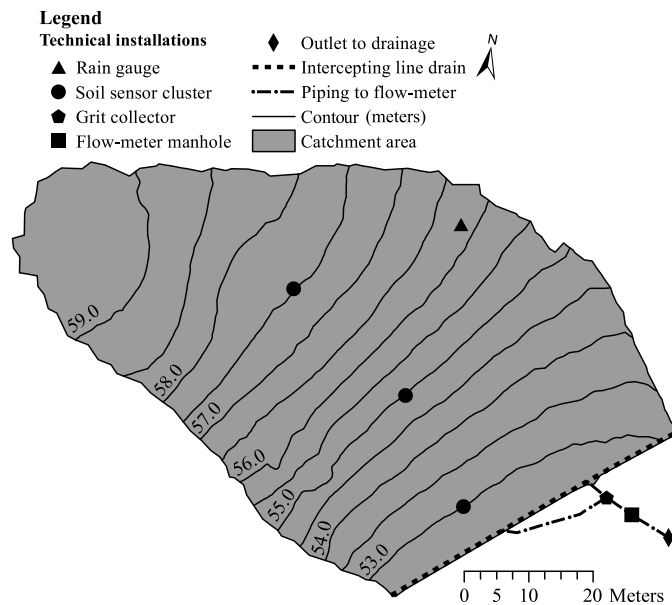


**Fig. 2.** Experimental location for field-scale observation of rainfall-runoff from an urban pervious area. Photographs from the established field station by Nielsen et al. (2019) is presented in (a–c): (a) a 51-m long line drain to collect pervious surface runoff; (b) a flow-meter to monitor the runoff rate; and (c) an uphill view of the runoff producing catchment.

temporary runoff spikes (Nielsen et al. 2019). Measurements did not record runoff with similar characteristics to infiltration excess runoff.

From previous studies, a linear relationship between accumulated runoff and rainfall from the measurement area is found if the soil volumetric water content for the site-specific soil is above 0.34 m<sup>3</sup> H<sub>2</sub>O/m<sup>3</sup> soil and if an initial loss of 7.1 mm is exceeded (interception of the  $x$ -axis in Fig. 4). This is described in Eq. (1) and Fig. 4 (Nielsen et al. 2019)

$$V(P) = 0.18P - 1.26 \quad (1)$$

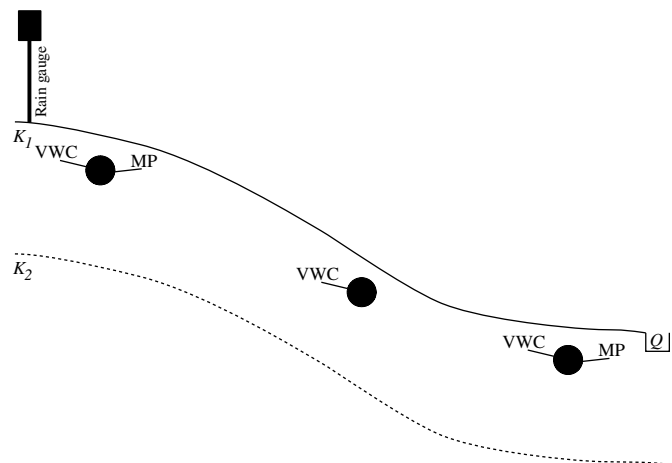
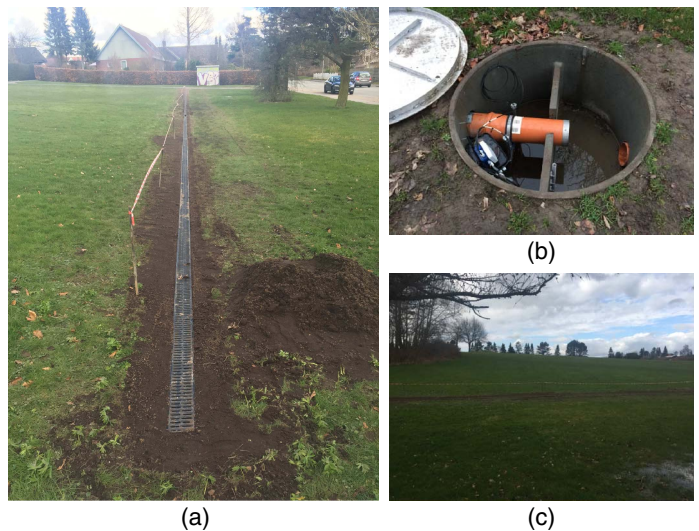


**Fig. 3.** Schematic profile drawing of sensor locations at the hill slope in Lystrup, Denmark. The solid line represents the soil surface while the dashed line illustrates the transition to the lower soil layer with the hydraulic conductivity  $K_2$ , which is lower than the hydraulic conductivity,  $K_1$ , of the upper soil layer. VWC and MP represents measurements of the soil volumetric water content and matric potential, while  $Q$  is the location of surface runoff collection. Rainfall is measured with the rain gauge.



where  $V$  = accumulated runoff [mm]; and  $P$  = accumulated rainfall [mm].

According to the slope of the linear regression in Eq. (1), the catchment has a runoff coefficient of  $\varphi = 0.18$  if the soil water content is above 0.34 m<sup>3</sup> H<sub>2</sub>O/m<sup>3</sup> soil and the initial loss of 7.1 mm is exceeded. In this way, infiltration is constant under highly saturated soil conditions in which 82% of the rainfall infiltrates.

The basic hydrological properties presented in Eq. (1) and Fig. 4 are used for further modeling and assumptions on when runoff is active. The assumptions are built into five different models, which are evaluated on their ability to simulate subsurface throughflow. First, the time-area and kinematic wave model are evaluated as these are typically used for modeling runoff in urban drainage engineering. The time-area and kinematic wave models assume that runoff transports directly on top of a surface. Additionally, a linear reservoir model and water-content based regression models are evaluated. These are typically used to estimate the discharge to rivers, assuming that water transport occurs horizontally in the topsoil and that water is later released to the river or surface. Finally, the capability of neural network models to simulate measured runoff is evaluated.

### Model 1: Time-Area Model

Using the time-area model for rainfall-runoff modeling with variable rainfall intensity, the catchment is divided into several subcatchments to simulate the effect of water retention on the catchment surface. The time-dependent hydrograph is calculated by Eq. (2) (Butler and Davies 2004)

$$Q(t) = \sum_{n=1}^{N_A} \Delta A_{(j)} i_{(n)} \varphi \quad (2)$$

where  $Q$  = outflow from the catchment [m<sup>3</sup> s<sup>-1</sup>];  $i_{(n)}$  [m s<sup>-1</sup>] = rainfall intensity in the  $n$ th [-] subcatchment cell with a duration of  $\Delta t$  [s];  $N_A$  = total number of subcatchment cells [-];  $\Delta A_{(j)}$  = surface area of the subcatchment cell contributing to runoff [m<sup>2</sup>];  $\varphi$  [-] = runoff coefficient; and  $j$  = subcatchment cell in which rainfall,  $i_n$ , precipitates. The value of  $j$  is calculated



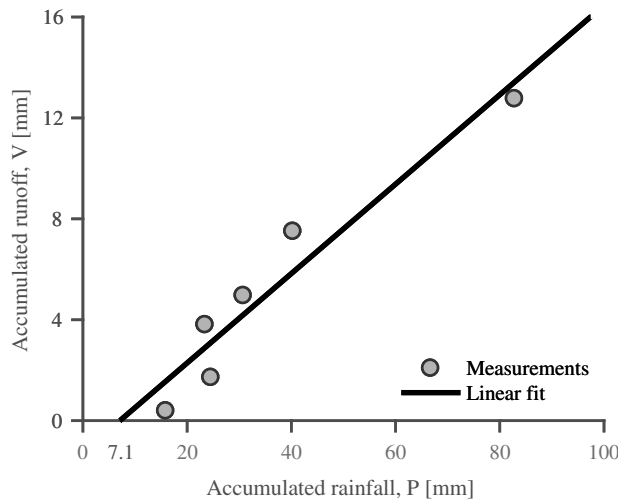


**Fig. 4.** Relationship between accumulated runoff and accumulated rainfall at soil volumetric water contents above  $0.34 \text{ m}^3 \text{ H}_2\text{O}/\text{m}^3$  soil.

$$j = t - (n - 1)\Delta t \quad (3)$$

The runoff coefficient is 0.18, as derived in Eq. (1), for soil water content conditions above  $0.34 \text{ m}^3 \text{ H}_2\text{O}/\text{m}^3$  soil. Under these soil water conditions, the infiltration to the lower soil layer is constant. Furthermore, no water is transferred to the time-area model if the soil volumetric water content from measured data is below  $0.34 \text{ m}^3 \text{ H}_2\text{O}/\text{m}^3$  soil. Additionally, when this soil water content level is reached, rainfall must still exceed an initial loss of 7.1 mm before runoff.

The value of  $N_A$  is calculated based on the concentration time,  $t_c$  [s], and chosen time increment duration,  $\Delta t$  (DHI 2010)

$$N_A = \frac{t_c}{\Delta t} \quad (4)$$

For traditional surface runoff models, the concentration time expresses the time water from the most distant area of the catchment takes to reach the catchment out. In this case, the concentration time expresses the transport time in the soil from the most distant uphill areas in the soil matrix. Assuming a rectangular catchment, the surface area increments are calculated

$$\Delta A_{(j)} = \frac{A}{N_A} \quad (5)$$

where  $A$  = total catchment surface area [ $\text{m}^2$ ].

### Model 2: Kinematic Wave Model

The physically-based kinematic wave model is based on the continuity equation and Manning's equation (Butler and Davies 2004). Assuming that flow is one-dimensional, the following continuity equation is formed of water storage in a catchment:

$$\frac{dy}{dt} = i(t)\varphi - \frac{Q(y, t)}{A} \quad (6)$$

where  $y$  = water depth in the catchment [m];  $t$  = time [s]; and  $i$  = rainfall intensity [ $\text{m s}^{-1}$ ]. Outflow from the catchment is calculated by Manning's equation (Munoz-Carpena et al. 1999)

$$Q(t) = BM y(t)^{5/3} I^{1/2} \quad (7)$$

where  $M$  = Manning's number [ $\text{m}^{1/3} \text{ s}^{-1}$ ];  $B$  = width of the flow channel or runoff contributing catchment [m]; and  $I$  = catchment slope [-].

Eq. (6) can be approximated in an explicit finite-difference scheme, assuming that the timestep  $\Delta t$  is small, so that the change in water depth  $y$  is approximately linear between timesteps

$$\frac{dy}{dt} = \frac{y_{(t+\Delta t)} - y_{(t)}}{\Delta t} \quad (8)$$

Now, substituting Eqs. (7) and (8) into Eq. (6) gives the kinematic wave approximation

$$y_{(t+\Delta t)} = \left( i_{(t)}\varphi - \frac{BM y_{(t)}^{5/3} I^{1/2}}{A} \right) \Delta t + y_{(t)} \quad (9)$$

Generally, it is assumed that no water ponds in the upper soil layer but infiltrates to deeper aquifer if the soil water content is below  $0.34 \text{ m}^3 \text{ H}_2\text{O}/\text{m}^3$  soil. If the soil water content level is exceeded, an initial loss of 7.1 mm must be still be exceeded before any ponding occurs in the upper soil layer.

### Model 3: Linear Reservoir Model

The linear reservoir model is also based on the continuity equation in Eq. (6). However, instead of relying on Manning's equation, the flow is linearly related to the water depth,  $y$ , with the proportionality constant,  $k_1$  [ $\text{m}^2 \text{ s}^{-1}$ ]. This results in the following approximation consisting of one reservoir:

$$\begin{cases} y_{(t+\Delta t)} = (P\varphi - \frac{k_1 y_{(t)}}{A}) \Delta t + y_{(t)} \\ Q_{(t+\Delta t)} = k_1 y_{(t+\Delta t)} \end{cases} \quad (10)$$

Like the kinematic wave model, no water ponds in the upper soil layer unless the soil water content is above  $0.34 \text{ m}^3 \text{ H}_2\text{O}/\text{m}^3$  soil, and the initial loss of 7.1 must be exceeded.

### Model 4: Regression Based Throughflow Model

It is investigated if simple regression models of catchment runoff as a function of soil water content can be used to estimate runoff. This is inspired by Kirkby and Chorley (1967) who presented a simple power function to simulate subsurface throughflow. The model defines the subsurface throughflow discharge as a function of soil water content exceeding a critical soil water content level at which water can no longer be stored in the soil

$$Q(\theta) = k_2(\theta - \theta_0)^{k_3} \quad (11)$$

where  $k_2$  and  $k_3$  = constants;  $\theta$  = measured soil water content of the catchment [ $\text{m}^3 \text{ H}_2\text{O}/\text{m}^3$  soil]; and  $\theta_0$  = soil water content level where the subsurface throughflow discharge is zero [ $\text{m}^3 \text{ H}_2\text{O}/\text{m}^3$  soil]. In this study,  $\theta_0$  is set to  $0.34 \text{ m}^3 \text{ H}_2\text{O}/\text{m}^3$  soil based on the relationship presented in Eq. (1) and Fig. 4. Furthermore, it is tested how a linear and exponential regression model performs compared to the power function given by Kirkby and Chorley (1967).

### Model 5: Two-Layer Feed-Forward Neural Network Model

A two-layer feed-forward neural network model, with the structure presented in Fig. 5, is tested to evaluate the quality of purely data-driven models. Two approaches are tested in the same network structure by using a different number of input variables. The two

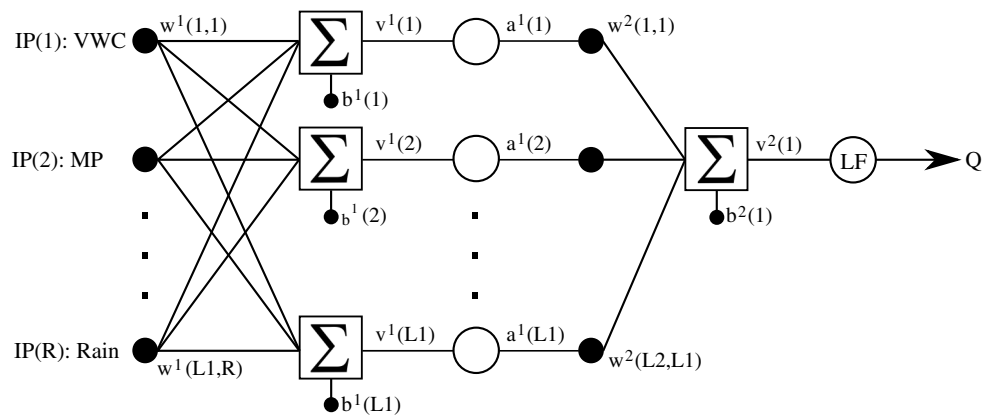


**Fig. 5.** Two-layer feed-forward neural network (Hagan and Menhaj 1994) trained on input  $R$  number of input variables,  $IP$ , to estimate catchment runoff,  $Q$ , in Lystrup, Denmark. In this case, the inputs consist of soil volumetric water content (VWC), soil matric potential (MP), and rainfall.

approaches are NN1, the *current data* approach, and NN2, the *past data* approach. The current data approach relies on the neural network trained to estimate the current catchment runoff,  $Q$ , based on the most recent observations of rainfall and soil-water properties. The current data approach has five input variables, which are (1) rainfall, (2) average soil water content in the catchment, (3) soil water content closest to the outlet of the catchment, (4) average soil matric potential in the catchment, and (5) soil matric potential closest to the outlet of the catchment. The input variables are measured at the same time as the catchment runoff,  $Q$ , which is the training target of the neural network. The past data approach includes the same data as the current data approach but also relies on the observations of the average soil water content in the catchment up until runoff. This means that the past data approach includes 6–17 input variables in which Input variables 1–5 are the same as the current data approach and Input variables 6–17 are the average soil water content in the catchment 15 min, 30 min, . . . 180 min behind the most recent observations. The input has no prior conditioning of when runoff is most probably active, and the network must therefore identify this relationship through training.

The neural network presented in Fig. 5 contains one hidden layer consisting of  $L1$  hidden, sigmoid-based neurons and one output layer consisting of one linear output neuron ( $L2 = 1$ ). The values of  $v^1$  and  $v^2$  are the weighted sums of the weight ( $w^1$  and  $w^2$ ) and bias ( $b^1$  and  $b^2$ ) corrected input variables,  $IP$ , to the respective neurons. The value of  $a^1$  is the output from the sigmoid function ( $\sigma$ ) in the hidden neurons and input data to the linear output neuron (Hagan and Menhaj 1994).

When training the network, the weights and biases in the network, as seen in Fig. 5, are adjusted using the Levenberg-Marquardt backpropagation (Marquardt 1963; Hagan and Menhaj 1994); however, not the full dataset is used for network training. To avoid overconditioning, 70% of the data are used for training, 15% are used for validation of the training process, and 15% are used for independent testing. The data is subdivided randomly for each network training. Technically, the difference between the training and validation data is that training data are used to optimize the weights and biases of the neural network while validation data are used to detect overfitting. During the training of the neural network, the fit of training and validation data will often converge. However, at some point, the validation data can be used to detect overfitting. That is, if the fit based on training data seems to improve but the fit based on validation data deteriorates, there is a sign of overfitting. In this case, weights and biases should be adjusted accordingly. After the training of the neural network model has

ended, the test data can be used to independently compare if these also fit the calibrated model without having been part of the training process.

## Performance Measures

The investigated models are evaluated based on three performance measures. First, the root mean square error (RMSE) is used to investigate deviations between observed and modeled data points (Ritter and Muñoz-Carpena 2013)

$$\text{RMSE} = \sqrt{\frac{\sum_{i=1}^N (O_i - M_i)^2}{N}} \quad (12)$$

where  $O_i$  = set of observation;  $M_i$  = modeled estimate; and  $N$  = sample size. The RMSE ranges from 0 to  $\infty$ , where 0 represents no deviation between the modeled fit and observed data.

Furthermore, the Nash-Sutcliffe efficiency (NSE) is calculated, given by Nash and Sutcliffe (1970) and Ritter and Muñoz-Carpena (2013)

$$\text{NSE} = 1 - \frac{\sum_{i=1}^N (O_i - M_i)^2}{\sum_{i=1}^N (O_i - \bar{O})^2} \quad (13)$$

The Nash-Sutcliffe efficiency ranges from  $-\infty$  to 1, where 1 is a perfect match between model and observations. If  $\text{NSE} = 0$ , the model is only as accurate as the mean of all the observations. If  $\text{NSE} < 0$ , the mean of the observations is a better predictor than the model itself.

Finally, the models are also tested in terms of the Bayesian likelihood ( $L$ ), which assumes a Gaussian distribution of observed and modeled data points (Beven and Freer 2001; Freer et al. 1996; Thorndahl et al. 2008)

$$L_i(O_i|M_i(\theta, I)) \propto \exp\left(\frac{-\sigma_{M_i-O_i}^2}{\sigma_{O_i}^2}\right) \quad (14)$$

where  $L$  = empirical likelihood;  $\theta$  = set of model parameters;  $I$  = model input variables;  $\sigma_{M_i-O_i}^2$  = variance of the error between modeled and observed data; and  $\sigma_{O_i}^2$  = variance of observed data. Due to the exponential of the variance ratio in Eq. (14), peak values of modeled and measured data have a larger impact on this performance indicator (Thorndahl et al. 2008). In this way,  $L$  is useful in terms of evaluating the different model's ability to simulate peak runoff values.

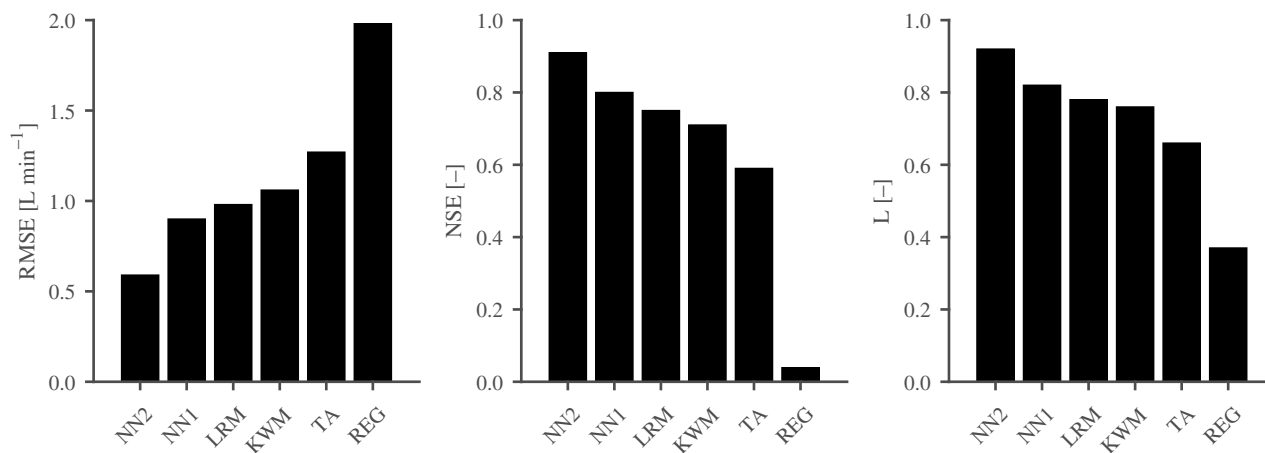


**Fig. 6.** Performance of the investigated models: regression models (REG), time-area model (TA), kinematic wave model (KWM), linear reservoir model (LRM), neural network using current data values (NN1), and neural network model implementing past data values (NN2).

## Results

The calibration and simulation of the presented models show large variations regarding modeling quality compared to measured data, as seen in Fig. 6. The neural network models have the best performance considering RMSE, NSE, and  $L$ . The neural network model based on current values of soil water content, matric potential, rainfall, and runoff to estimate the current runoff rate from the experimental catchment show that the best fit is found using 32 neurons in the hidden layer (RMSE = 0.90  $L \min^{-1}$ , NSE = 0.80, and  $L = 82$ ). An implementation of past data values in the same neural network structure increases the modeling precision of the runoff. Using past data up to 180 min before the current time and a neural network containing 60 neurons results in the best performance (RMSE = 0.59  $L \min^{-1}$ , NSE = 0.91, and  $L = 92$ ).

According to Fig. 6, the kinematic wave and linear reservoir models also show a relatively good performance in terms of simulating measured runoff (RMSE = 1.06  $L \min^{-1}$ , NSE = 0.71, and  $L = 0.76$  for the kinematic wave model, and RMSE = 0.98  $L \min^{-1}$ , NSE = 0.75, and  $L = 0.78$  for the linear reservoir model). The time-area model has a slightly lower performance (RMSE = 1.27  $L \min^{-1}$ , NSE = 0.59, and  $L = 0.66$ ). Finally, the regression-based throughflow models show the worst performance (RMSE = 1.98  $L \min^{-1}$ , NSE = 0.03, and  $L = 0.37$ ). According to the NSE performance, the predictability of the model is very limited.

The optimal concentration time for the time-area model was found to be long,  $t_c = 3,175$  min. Consequently, the model also contains a large number of subcatchments. Although the concentration time might not be physically meaningful in the traditional context of the time-area model, the large numerical value makes the model able to predict the measured long-lasting subsurface throughflow with some accuracy. The computed runoff of the time-area model is illustrated in Fig. 7 and shows that the model results in flat peak values, which do not correspond to occurring peaks in the measured data. However, the time-area model seems to have some accuracy in modeling the delayed effects of measured runoff.

The optimal Manning number for the kinematic wave model was found to be  $M = 8.94 \text{ m}^{1/3} \text{ min}^{-1}$  ( $0.15 \text{ m}^{1/3} \text{ s}^{-1}$ ), which corresponds to a very high surface roughness not typically used for urban pervious surfaces. The Manning number is not physically feasible, but its low numerical value gives the kinematic wave model a reasonable performance. In this way, Manning's number

becomes a calibration constant instead of an expression of surface roughness, which contains other important variables that could be related to the permeability of the soil. In Fig. 7, it is seen that the kinematic wave model is better at simulating the runoff peaks and the long-term tailing of the measured runoff compared to the time-area model. However, it is difficult for the kinematic wave model to capture the strongest runoff peaks.

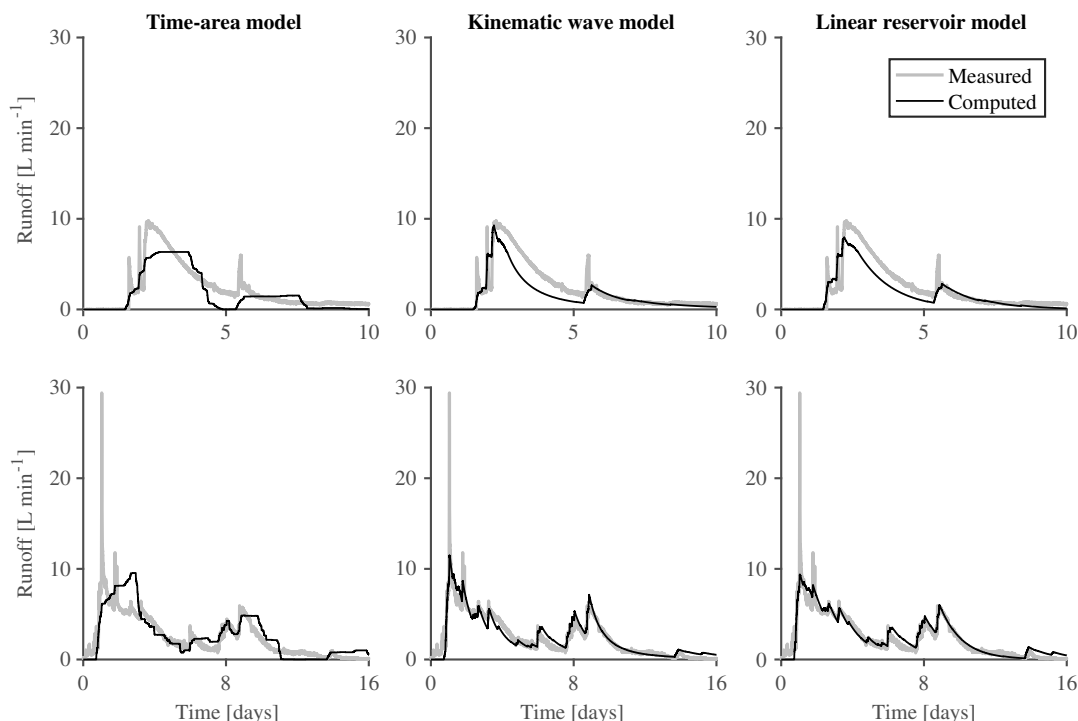
The calibrated linear reservoir model has a proportionality constant of  $2.46 \text{ m}^2 \text{ min}^{-1}$  and obtains similar results to the kinematic wave model. However, the linear reservoir model has a slightly better modeling performance according to the performance measures. Nonetheless, the model cannot predict the strongest runoff peaks.

No correlation was found directly between the measured runoff and measured soil water content excess ( $\theta - \theta_0$ ) in the regression-based subsurface throughflow models. The reason for this is that runoff starts at different levels of soil water content excess. This makes a general regression-model unsuitable for simulating the measured runoff in this case.

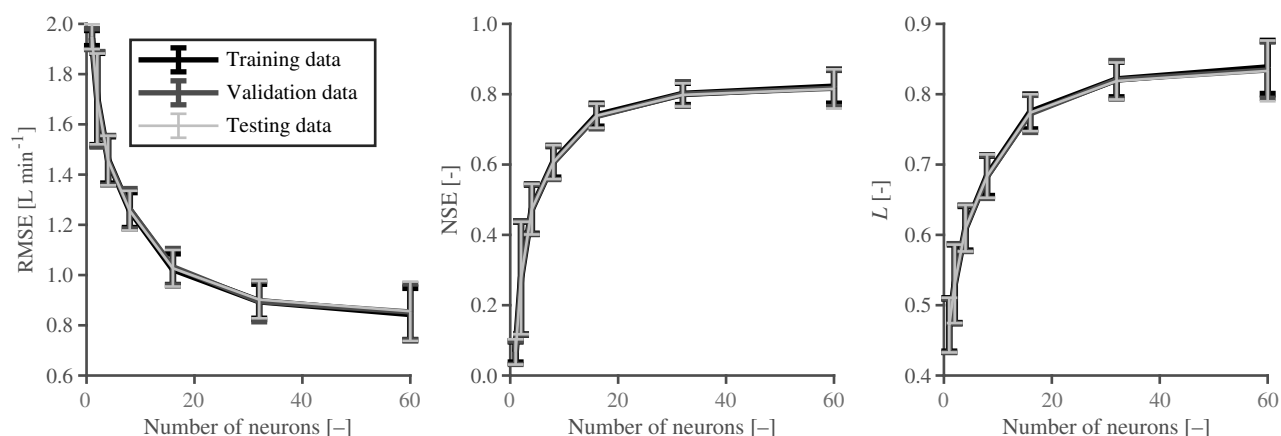
The shallow neural network model based on current data to estimate current runoff values reproduced measured runoff with different qualities, depending on the number of neurons included, as presented in Fig. 8. In terms of RMSE, NSE, and  $L$ , the modeling performance increased with an increased number of neurons in the network. However, the improvement seems to become smaller with more neurons included in the network. The standard deviation of RMSE, NSE, and  $L$  seems to increase using 60 neurons, while the smallest standard deviations in the modeling performance are found using between 16 and 32 neurons. The increase in the standard deviation using 60 neurons could indicate the risk of an overconditioning of the network. Therefore, using 32 neurons in the neural network is considered the most reliable solution in this case.

Fig. 9 shows that simulated runoff behaves differently depending on the number of neurons. It is seen that by using 32 and 60 neurons, the neural network is somewhat better at simulating the stronger, short-term, peaks at the start of the event. Furthermore, with increasing the number of neurons, the simulated runoff increasingly overlaps with the measured runoff. However, increasing the number of neurons in the network also produces sudden fluctuations more frequently, which are not seen within the measured data.

The modeling performance by implementing past data in the neural network training is illustrated in Fig. 10. In this way, it is possible to increase the modeling performance compared to only



**Fig. 7.** Comparison of measured runoff and runoff dynamics computed by the time-area method, kinematic wave model, and linear reservoir model to two measured rainfall-runoff events. The upper event was measured from November 4, 2016, to November 14, 2016, and the lower event was measured from September 5, 2017, to September 22, 2017.



**Fig. 8.** Change in the average RMSE, NSE, and  $L$  based on the number of neurons included in the hidden layer of the neural network based on current data values. The average value for each set of neurons is based on 100 separate simulations where a neural network is trained. Error bars illustrate the standard deviation of the 100 simulations.

using current data as input. The performance is generally increasing with more data from the past included and the increased number of neurons in the network. The best neural network in this case contains 60 neurons and 180 min of data up until the runoff estimate.

Fig. 11 clearly illustrates the added benefit of including past data into the neural network, as it stabilizes the model output and increases the model performance with significantly better peak prediction.

## Discussion

The models tested in this study show differences in the quality of simulating the runoff from the experimental site, as illustrated by

the performance measures. Generally, the performance measures are correlated, which means that RMSE, NSE, and  $L$  agrees on the performance ranking of the models. The neural network models have the best performance. Furthermore, including past data into the neural network improves modeling performance even more. However, the more physically based kinematic wave model and linear reservoir model also seem to have a reasonably good performance compared to the neural network models. The time-area model has some capability of modeling subsurface throughflow. However, there seems to be a limitation in simulating peak runoff values. It should be noted that the performance of the kinematic wave and time area model is based on calibrated values of the Manning's number and the concentration time, which obtains



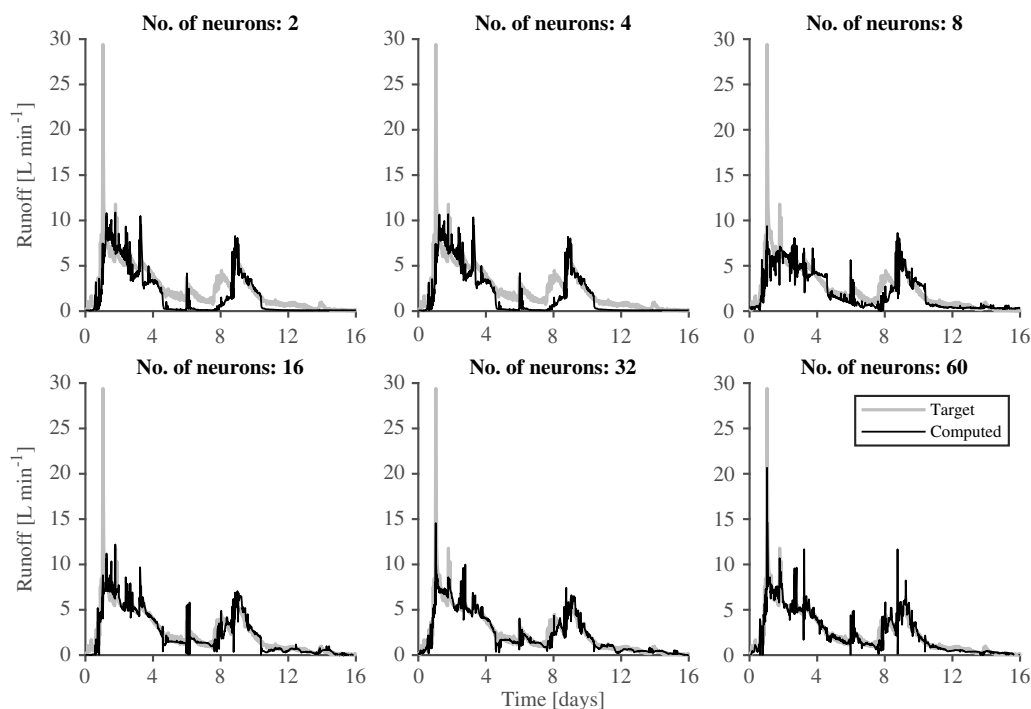


**Fig. 9.** Dynamics of optimized neural networks compared to measured runoff. The optimized neural networks with 2–60 neurons in the hidden layer are presented. The measured runoff started September 5, 2017 and ended September 22, 2017.

physically unrealistic values. Finally, in this case, regression-based runoff models are not suitable to simulate subsurface throughflow as there is no direct correlation between runoff and the soil water content excess ( $\theta - \theta_0$ ).

The high concentration time of the time-area model and low Manning's number of the kinematic wave model show that there is high retention of water in the catchments surface. This demonstrates that the runoff processes are dominated by subsurface throughflow and, thereby, runoff horizontally in the soil, which automatically introduces resistance to the water movement. Generally, the time-area and kinematic wave model are normally used for runoff modeling directly on pervious or impervious surfaces. However, in this case, the high concentration time and low Manning's number are sufficient parameters to calibrate to include more detention of water in the system. Although these models obtain physically unrealistic model parameter values regarding free water flow on the surface, it seems that it is possible to use them to simulate subsurface throughflow with a relatively high accuracy. This could be useful for urban drainage engineers as these are the primary models typically included in commercially available urban drainage models. Therefore, by adjusting the model parameters, it is possible to include subsurface throughflow as a contributor of surface runoff to drainage systems with traditional models that are widely available. This could be of value for urban drainage engineers but will require more research to be done on methods for establishing the model parameters without extensive instrumentation of specific sites.

The consequence of the model optimization in this study is that the models are very likely only to fit the runoff at the experimental catchment. Furthermore, the sensitivity of the time-area model, kinematic wave model, and linear reservoir model to the parameters used for optimization is relatively high, as illustrated in Fig. 12. The models generally have a relatively small interval with a high-modeling precession. This emphasises the importance of calibration based on measured data to obtain accurate and reliable model results.

Aside from the neural network models, the kinematic wave model and linear reservoir model are the best models to simulate the measured runoff. The reason for this is most probably because both models are based on the continuity equation. In this way, both models include a storage term ( $dy/dt$ ), which expresses the amount of rainfall stored within the soil. Therefore, the storage term could be the most important physical term to give a good representation of the actual physics of the measured runoff in the experimental area. This is also the physical principle the regression-based models exploit based on measured soil water content, thus, with less success in this study. However, the number of points in which the soil water content is measured might be too low to give a sufficient estimate of the current storage of water in the catchment both horizontally and vertically.

The neural network models perform the best. However, there is a tendency with an increased number of neurons that the networks produce more fluctuations in simulated runoff, which seem uncorrelated to measured runoff. This could be a result of overfitting, although the average RMSE, NSE, and  $L$  of the training, validation, and test data are close according to Fig. 8. This generally means that there is a risk with an increasing number of neurons that the neural networks are only suitable to simulate runoff within the time frame it has been fed with data. It is seen that the performance of the neural network increases using past observations. This is most likely because by including past observations, a memory is included similar to the storage term of the continuity equation in the kinematic wave and linear reservoir model. Furthermore, implementing past observations in the neural network also reveal at which rate the soil water content has increased or decreased prior to the current time. In this way, for example, if the prior four points of measured soil water content have increased rapidly, there might also be a chance that the runoff rate should increase rapidly.

All applied models in this study have difficulties simulating short-term and high-peak runoff rates. Generally, this is because

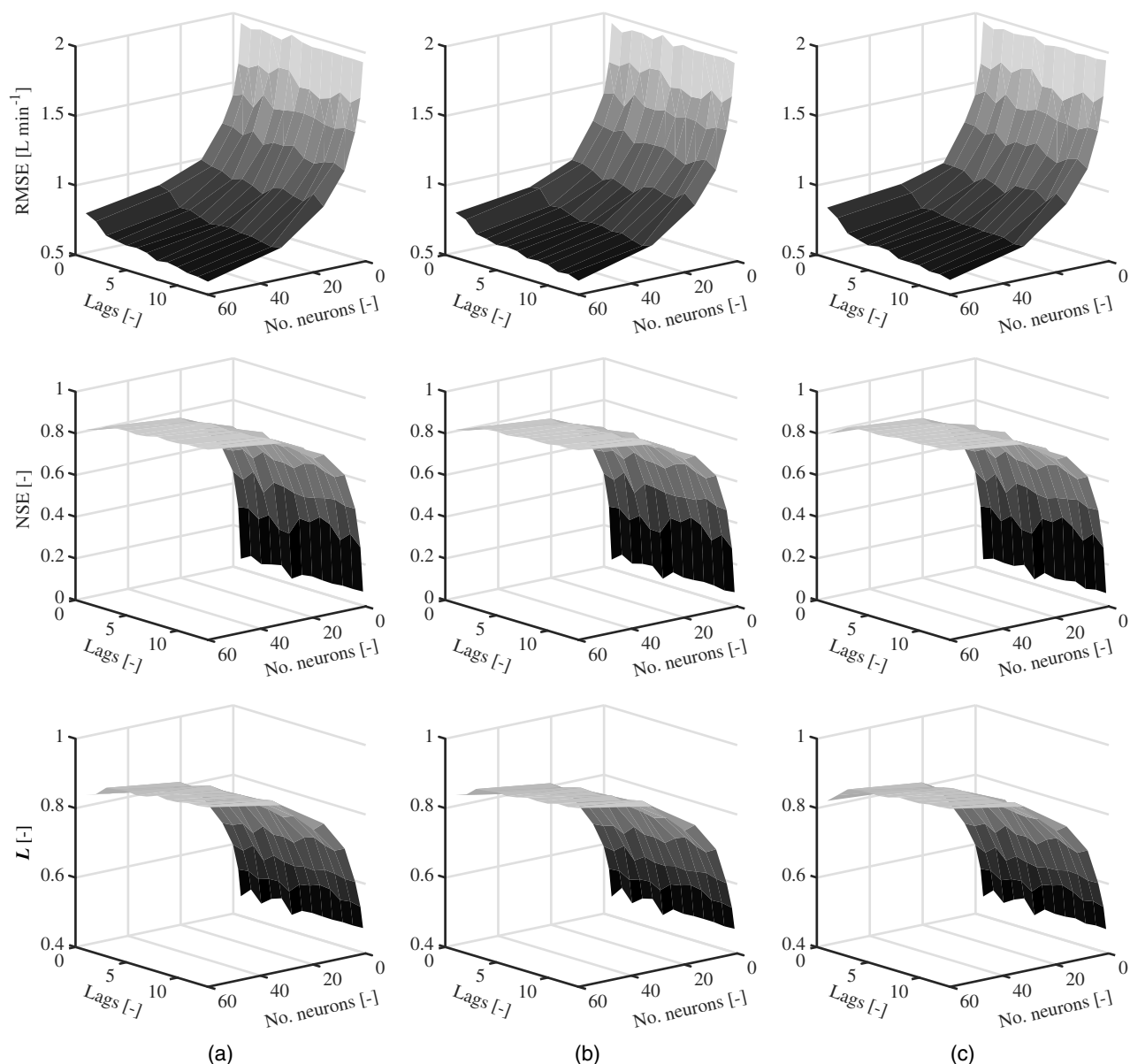


**Fig. 10.** RMSE, NSE, and  $L$  of neural network trained using an increasing number of neurons and amount of past data (data lags): (a) the error of the training dataset; (b) the error of the validation dataset; and (c) the error of the test dataset. If lag = 1, only current data are used; if lag = 2, current data and data 15 min back are used. If lag = 13, current data, and data at 15 min, 30 min, . . . 180 min back are used for the network training: (a) training; (b) validation; and (c) test.

these strong runoff peaks are caused by saturation excess overland flow, which only represents a very small part of the entire dataset. Therefore, it is not possible to produce any reasonable fit for this type of runoff. However, the neural network handles this runoff type to some degree when a higher number of neurons are included in the network. If saturation excess runoff should be included in the time-area, kinematic wave, and linear reservoir models, this would require multilayered models to separate the two types of runoff as these are physically very different processes. However, there is not enough data available on saturation excess overland flow to make any reasonable model fit for this type of flow. Ideally, this type of flow should be further considered, as it is seen that it can significantly increase the runoff rate from the experimental catchment over short periods (Nielsen et al. 2019).

This study shows that the kinematic wave and linear reservoir models perform comparably to the neural network using current

data in terms of RMSE, NSE, and  $L$ ; however, the kinematic wave and linear reservoir models are more stable. Additionally, they require only one parameter to be calibrated to obtain a reasonable fit, while the neural network models require adjustment of several weights and biases proportionally to the number of neurons in the network. Furthermore, the neural network models are completely data-driven, and therefore, no physical meaning is built into these models. Hence, in this case, it could be more reliable to use kinematic wave and linear reservoir models if these models should give a good physical representation of reality.

In the study by Nielsen et al. (2019), it was concluded that runoff did not occur at soil volumetric water contents smaller than  $0.34 \text{ m}^3 \text{ H}_2\text{O}/\text{m}^3 \text{ soil}$ . Additionally, accumulated runoff was linearly correlated to accumulated rainfall, yielding a runoff coefficient of 0.18. This provides very clear definitions of when runoff is most likely present and how much runoff can be expected

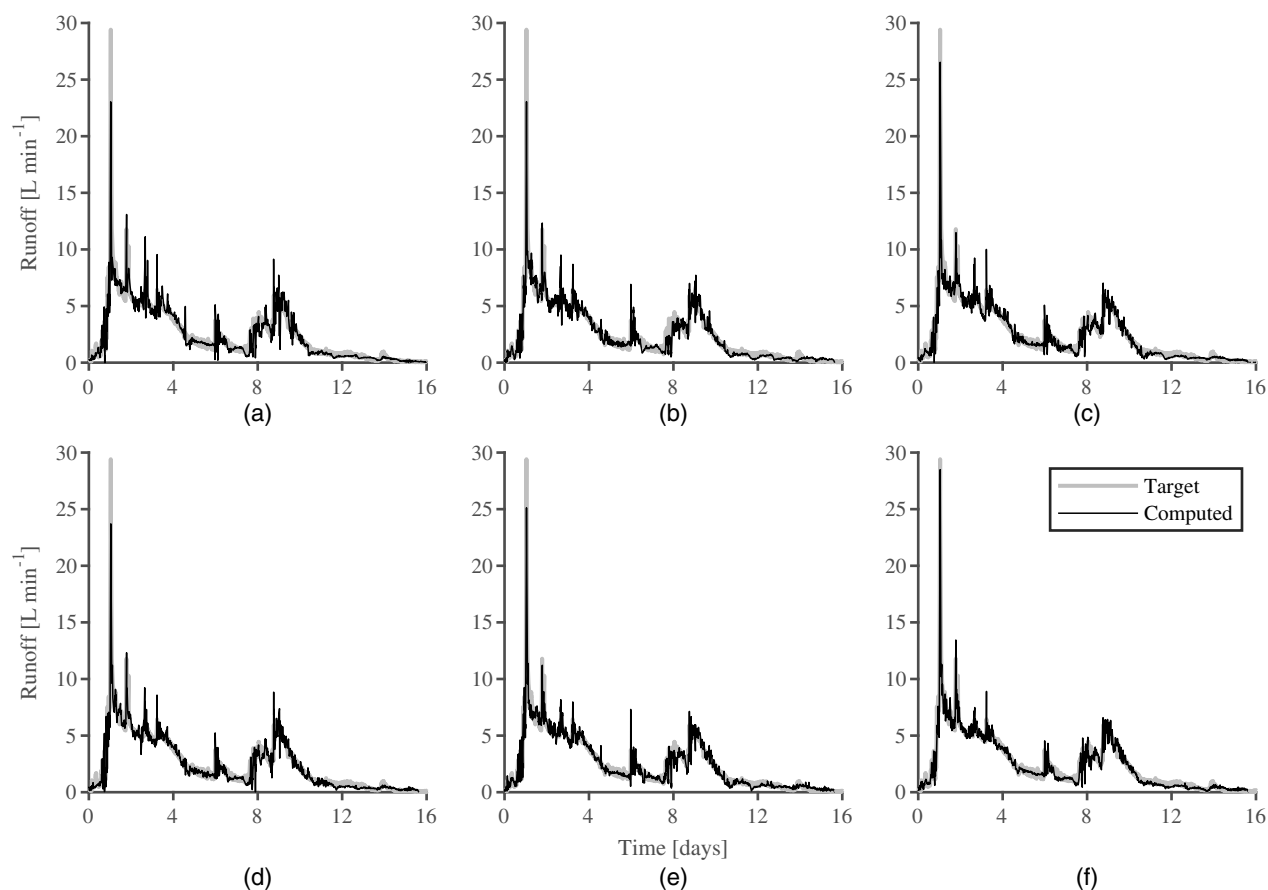


**Fig. 11.** Dynamics of optimized neural networks including different number of delayed input data in terms of soil water content: (a–f) illustrate the dynamics of simulated runoff using 30 to 180 min delayed soil water content. The measured runoff started September 5, 2017 and ended September 22, 2017: (a) Lags: 15 and 30 min; (b) Lags: 15, 30, ... 60 min; (c) Lags: 15, 30, ... 90 min; (d) Lags: 15, 30, ... 120 min; (e) Lags: 15, 30, ... 150 min; and (f) Lags: 15, 30, ... 180 min.

(18% of accumulated rainfall) at soil water contents above this level. Had this relationship not been available, it would not have been possible to obtain the same accuracy of the calibrated time-area, kinematic wave, and linear reservoir models as presented in this study. In such cases, a neural network could be effectively employed to derive a mathematical model for simulating runoff as a function of soil water properties and rainfall.

The primary focus of this paper is to investigate the applicability of traditional surface runoff models used in urban drainage engineering. However, future studies could investigate the use of soil-water transport models, such as a two-dimensional numerical Darcy model to simulate the vertical and horizontal flow recorded at the project location (Rassam et al. 2003). This kind of model would represent the actual nature of the project location better but is rarely used in urban drainage engineering. Furthermore, other empirical models, such as the runoff curve number method (Ponce and Hawkins 1996), could be included in future studies to investigate the potential of other simplistic models to replicate the measured results.

## Practical Applications

This study shows that widely applied models in urban drainage engineering can be adjusted to meet the requirements necessary to make a satisfactorily estimate of subsurface throughflow from a

catchment in Lystrup, Denmark. The obtained model parameter values of the concentration time and the Manning number are unrealistic and could potentially only be useful to simulate runoff from the specific location. Therefore, to investigate if these parameters are applicable in a global sense, there is a need for more experimental studies. More experiments will also indicate the actual need for models to simulate subsurface throughflow in urban hydrology. This will help to assess the global applicability of current runoff models to simulate subsurface throughflow and how subsurface throughflow affects drainage systems on a broader scale. Furthermore, this study cannot stand alone for generalization, as different soil types, surface slopes, vegetation, and so forth will affect runoff differently and, thereby, generate a large spatial variability.

## Conclusion

It is found that it is possible to simulate measured subsurface throughflow from an experimental catchment in Lystrup, Denmark. In introducing a high surface roughness in the kinematic wave model, the model produces reasonable results in simulating subsurface throughflow. Furthermore, a linear reservoir model gave similar results and showed a good performance. Neural network models, including past data up to 180 min old, resulted in a better performance compared to neural networks based only on current data. The time-area model has some issues in terms of modeling

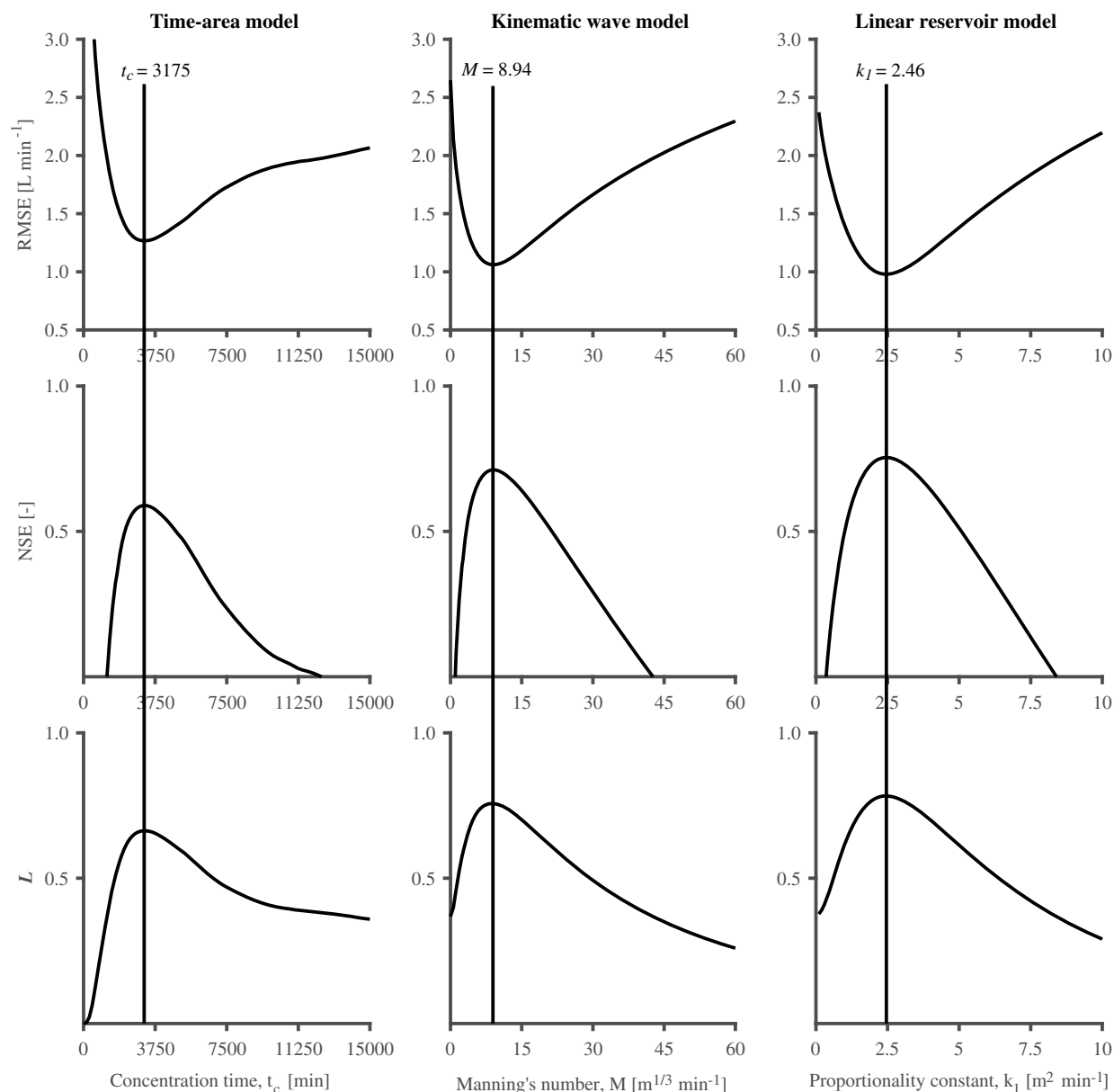


**Fig. 12.** Sensitivity analysis of optimized parameters of the time-area model, kinematic wave model, and linear reservoir model.

the correct dynamics of subsurface throughflow. Therefore, the time-area model only has limited use to simulate this type of runoff. Finally, regression-based subsurface throughflow models based on the soil water content excess show no reasonable fit and cannot be used for modeling the subsurface throughflow from the experimental catchment in this study. Generally, the neural network model, including past data, have the best performance of all tested models. However, the linear reservoir model might be the best compromise in terms of model complexity and performance.

### Data Availability Statement

Some or all data, models, or code generated or used during the study are available from the corresponding author by request. This includes (1) the measurement data on rainfall, soil-water properties, and runoff and (2) scripts and function to filter raw data and scripts with the models presented in this paper.

### Acknowledgments

This research was partially funded by The Foundation for Development of Technology in the Danish Water Sector, the Innovation Fund Denmark, Aarhus Vand, EnviDan A/S, and Aalborg University.

### References

- ASCE Task Committee on Application of Artificial Neural Networks in Hydrology. 2000. "Artificial neural networks in hydrology. II: Hydrologic applications." *J. Hydrol. Eng.* 5 (2): 124–137. [https://doi.org/10.1061/\(ASCE\)1084-0699\(2000\)5:2\(124\)](https://doi.org/10.1061/(ASCE)1084-0699(2000)5:2(124)).
- Ashman, M., and G. Puri. 2013. *Essential soil science: A clear and concise introduction to soil science*. New York: Wiley.
- Beven, K., and J. Freer. 2001. "Equifinality, data assimilation, and uncertainty estimation in mechanistic modelling of complex environmental systems using the GLUE methodology." *J. Hydrol.* 249 (1–4): 11–29. [https://doi.org/10.1016/S0022-1694\(01\)00421-8](https://doi.org/10.1016/S0022-1694(01)00421-8).



- Butler, D., and J. W. Davies. 2004. *Urban drainage*. Boca Raton, FL: CRC Press.
- Celia, M. A., E. T. Bouloutas, and R. L. Zarba. 1990. "A general mass-conservative numerical solution for the unsaturated flow equation." *Water Resour. Res.* 26 (7): 1483–1496. <https://doi.org/10.1029/WR026i007p01483>.
- DHI (Danish Hydraulic Institute). 2010. *Mouse surface runoff models—Reference manual*. New Delhi, India: DHI.
- Dunne, T., and R. D. Black. 1970a. "An experimental investigation of runoff production in permeable soils." *Water Resour. Res.* 6 (2): 478–490. <https://doi.org/10.1029/WR006i002p00478>.
- Dunne, T., and R. D. Black. 1970b. "Partial area contributions to storm runoff in a small New England watershed." *Water Resour. Res.* 6 (5): 1296–1311. <https://doi.org/10.1029/WR006i005p01296>.
- Freer, J., K. Beven, and B. Ambrose. 1996. "Bayesian estimation of uncertainty in runoff prediction and the value of data: An application of the GLUE approach." *Water Resour. Res.* 32 (7): 2161–2173. <https://doi.org/10.1029/95WR03723>.
- Govindaraju, R. S. 2000. "Artificial neural networks in hydrology. I: Preliminary concepts." *J. Hydrol. Eng.* 5 (2): 115–123. [https://doi.org/10.1061/\(ASCE\)1084-0699\(2000\)5:3A2\(115\)](https://doi.org/10.1061/(ASCE)1084-0699(2000)5:3A2(115)).
- Green, W. H., and G. A. Ampt. 1911. "Studies on soil physics." *J. Agric. Sci.* 4 (1): 1–24. <https://doi.org/10.1017/S0021859600001441>.
- Gregory, J. H. 2006. "Effect of urban soil compaction on infiltration rate." *J. Soil Water Conserv.* 61 (3): 117–124.
- Groenendyk, D. G., T. P. A. Ferré, K. R. Thorp, and A. K. Rice. 2015. "Hydrologic-process-based soil texture classifications for improved visualization of landscape function." *PLoS One* 10 (6): e0131299. <https://doi.org/10.1371/journal.pone.0131299>.
- Hagan, M. T., and M. B. Menhaj. 1994. "Training feedforward networks with the Marquardt algorithm." *IEEE Trans. Neural Netw.* 5 (6): 989–993. <https://doi.org/10.1109/72.329697>.
- Horton, R. E. 1939. "Analysis of runoff-plat experiments with varying infiltration-capacity." *Eos Trans. Am. Geophys. Union* 20 (4): 693–711. <https://doi.org/10.1029/TR020i004p00693>.
- Jacobs, J. M., D. A. Myers, and B. M. Whitfield. 2003. "Improved rainfall/runoff estimates using remotely sensed soil moisture." *J. Am. Water Resour. Assoc.* 39 (2): 313–324. <https://doi.org/10.1111/j.1752-1688.2003.tb04386.x>.
- Kirkby, M. J., and R. J. Chorley. 1967. "Throughflow, overland flow and erosion." *Bull. Int. Assoc. Sci. Hydrol.* 12 (3): 5–21. <https://doi.org/10.1080/02626666709493533>.
- Marquardt, D. W. 1963. "An algorithm for least-squares estimation of nonlinear parameters." *J. Soc. Ind. Appl. Math.* 11 (2): 431–441. <https://doi.org/10.1137/0111030>.
- Morris, E. M., and D. A. Woolhiser. 1980. "Unsteady one-dimensional flow over a plane: Partial equilibrium and recession hydrographs." *Water Resour. Res.* 16 (2): 355–360. <https://doi.org/10.1029/WR016i002p00355>.
- Munoz-Carpena, R., J. E. Parsons, and J. W. Gilliam. 1999. "Modeling hydrology and sediment transport in vegetative filter strips." *J. Hydrol.* 214 (1–4): 111–129.
- Nash, J. E., and J. V. Sutcliffe. 1970. "River flow forecasting through conceptual models. Part I—A discussion of principles." *J. Hydrol.* 10 (3): 282–290. [https://doi.org/10.1016/0022-1694\(70\)90255-6](https://doi.org/10.1016/0022-1694(70)90255-6).
- Nielsen, K. T., P. Moldrop, S. Thorndahl, J. E. Nielsen, M. Uggerby, and M. R. Rasmussen. 2019. "Field-scale monitoring of urban green area rainfall-runoff processes." *J. Hydrol. Eng.* 24 (8): 04019022. [https://doi.org/10.1061/\(ASCE\)HE.1943-5584.0001795](https://doi.org/10.1061/(ASCE)HE.1943-5584.0001795).
- Pan, C., and Z. Shanguan. 2006. "Runoff hydraulic characteristics and sediment generation in sloped grassplots under simulated rainfall conditions." *J. Hydrol.* 331 (1–2): 178–185. <https://doi.org/10.1016/j.jhydrol.2006.05.011>.
- Pedersen, J. T., J. C. Peters, and O. J. Helweg. 1980. *Hydrographs by single linear reservoir model*. Davis, CA: Hydrologic Engineering Center.
- Pilgrim, D. H., D. D. Huff, and T. D. Steele. 1978. "A field evaluation of subsurface and surface runoff." *J. Hydrol.* 38 (3–4): 319–341. [https://doi.org/10.1016/0022-1694\(78\)90077-X](https://doi.org/10.1016/0022-1694(78)90077-X).
- Ponce, V. M., and R. H. Hawkins. 1996. "Runoff curve number: Has it reached maturity?" *J. Hydrol. Eng.* 1 (1): 11–19. [https://doi.org/10.1061/\(ASCE\)1084-0699\(1996\)1:1\(11\)](https://doi.org/10.1061/(ASCE)1084-0699(1996)1:1(11)).
- Quinton, J. N., G. Edwards, and R. Morgan. 1997. "The influence of vegetation species and plant properties on runoff and soil erosion: Results from a rainfall simulation study in south east Spain." *Soil Use Manage.* 13 (3): 143–148. <https://doi.org/10.1111/j.1475-2743.1997.tb00575.x>.
- Rassam, D., J. Simunek, and M. T. Van Genuchten. 2003. *Modelling variably saturated flow with HYDRUS-2D*. Brisbane, Australia: ND Consult.
- Ritter, A., and R. Muñoz-Carpena. 2013. "Performance evaluation of hydrological models: Statistical significance for reducing subjectivity in goodness-of-fit assessments." *J. Hydrol.* 480 (Feb): 33–45. <https://doi.org/10.1016/j.jhydrol.2012.12.004>.
- Sharma, K. D. 1986. "Runoff behaviour of water harvesting microcatchments." *Agric. Water Manage.* 11 (2): 137–144. [https://doi.org/10.1016/0378-3774\(86\)90026-0](https://doi.org/10.1016/0378-3774(86)90026-0).
- Tayfur, G., M. L. Kavvas, R. S. Govindaraju, and D. E. Storm. 1993. "Applicability of St. Venant equations for two-dimensional overland flows over rough infiltrating surfaces." *J. Hydraul. Eng.* 119 (1): 51–63. [https://doi.org/10.1061/\(ASCE\)0733-9429\(1993\)119:1\(51\)](https://doi.org/10.1061/(ASCE)0733-9429(1993)119:1(51)).
- Thorndahl, S., K. J. Beven, J. B. Jensen, and K. Schaarp-Jensen. 2008. "Event based uncertainty assessment in urban drainage modelling, applying the GLUE methodology." *J. Hydrol.* 357 (3–4): 421–437. <https://doi.org/10.1016/j.jhydrol.2008.05.027>.